Macromolecules
ARTICLE

Macromolecules **2009**, *42*, 7091–7097 **7091**
DOI: 10.1021/ma901122s

Polymer Diffusion Exhibits a Minimum with Increasing Single-Walled Carbon Nanotube Concentration

Minfang Mu,[†] Nigel Clarke,[‡] Russell J. Composto,[†] and Karen I. Winey*,[†]

[†]*Department of Materials Science and Engineering, University of Pennsylvania, Philadelphia, Pennsylvania 19104-6272, and* [‡]*Department of Chemistry, Durham University, Durham DH1 3LE, United Kingdom*

Received May 22, 2009; Revised Manuscript Received August 6, 2009

ABSTRACT: Nanoparticles present a new frontier for understanding polymer dynamics in complex, nanoscale environments. We report that the addition of single-walled carbon nanotubes (SWCNTs) produces a minimum in the diffusion coefficient with increasing nanoparticle concentration, ϕ. Initially, tracer diffusion coefficients (D) are suppressed with increasing ϕ and then increase beyond a critical concentration, $\phi_{crit} < 1$ vol %. Shorter tracer chains exhibit a greater slowing down than longer chains, whereas longer matrix chains decrease the value of ϕ_{crit}. The experimental results are discussed in terms of locally anisotropic diffusion perpendicular and parallel to the nanotube filler and simulated using a trap model that defines a trap size and the extent of slowing perpendicular to the cylindrical trap. The simulated diffusion coefficients capture both the initial decrease in D attributed to isolated traps and the recovery of D above ϕ_{crit} corresponding to trap percolation. Nanoparticles influence polymer diffusion in fascinating ways and will refine our understanding of polymer reptation and might also inform the study of biopolymer diffusion in living systems.

1. Introduction

In 1855, Fick surmised that the flow of matter is analogous to the flow of heat and electricity and proposed that the flux of matter is proportional to its concentration gradient and later the chemical potential gradient.[1,2] Fick's first law persists as *the* model for determining macroscopic diffusion coefficients. Subsequently, the atomic and molecular scale mechanisms of diffusion have been elucidated starting with Einstein's 1906 work on liquids[3] and more recently with de Gennes' 1971 reptation mechanism for polymer melts.[4] The reptation model describes the motion of a polymer along its contour as it passes the physical constraints imposed by the surrounding polymers and predicts the molecular weight dependence of the macroscopic diffusion coefficient. Polymer diffusion studies first focused on simple linear chains in matrices of equally simple polymers,[5,6] while subsequent studies explored more complex architectures including branched molecules, star molecules, and loops.[5,7−10]

Here we investigate the diffusion of linear polymers in the presence of nanoparticles. Nanoparticles with desirable properties are now widely available, and there has been an explosion of activities focused on combining nanoparticles with polymers to create polymer nanocomposites with unique and valuable properties.[11−13] Nanoparticles also provide access to a new range of size differences between particles and polymers, wherein the radius of gyration (R_g) of the polymer is considerably larger than the nanoparticle. For example, C_{60} fullerenes have diameters of 0.7 nm and a polystyrene (PS) of 75 000 g/mol molecular weight has $2R_g = 15$ nm.

The addition of nanoparticles to polymers provides a new challenge to building a fundamental understanding of polymer dynamics in complex environments. In the example of C_{60} and PS, one might predict that the addition of the nanoparticles to a polymer would act as a diluent and thereby smoothly increase both the free volume of the system and the diffusion coefficient as the fullerene concentration increases. In contrast, this study reports that the addition single-walled carbon nanotubes (SWCNTs) produces a minimum in the diffusion coefficient with increasing nanoparticle concentration. Thus, the addition of nanoparticles to polymers has unforeseen consequences on polymer diffusion, which in turn has direct impact on practical problems, such as the stability of nanoparticle dispersions.

Since the 1980s, elastic recoil detection (ERD) has been used to study polymer diffusion[14] and thereby played a key role in testing leading polymer diffusion theories including reptation, constraint release, and mutual diffusion.[5,15,16] ERD is an ion beam technique that directly provides a concentration profile of diffusing species, typically a deuterated polymer, as a function of depth into a matrix. Polymer dynamics can also be explored using rheology, but this is limited to nanocomposites with low nanoparticle concentrations to avoid solidlike behavior.[17] Gas permeability can indirectly probe polymer dynamics but is inappropriate when using SWCNTs because small molecules can be transported inside carbon nanotubes.[18,19] Using ERD, we follow tracer diffusion of deuterated polystyrene (dPS) in polystyrene (PS) nanocomposites to understand the influence of SWCNTs on polymer dynamics. This new understanding will enable better manipulation of polymer nanocomposite properties and melt processing, and could impact our understanding of macromolecular movement in living cells.[20,21]

2. Experimental Methods

2.1. Materials. Single-walled carbon nanotubes were synthesized by a high-pressure carbon monoxide conversion (HiPco) method at Rice University. Raw SWCNTs were purified by thermal oxidization and a HCl treatment.[22] The residual metal is < 5 wt %, as measured by TGA. Polystyrenes (PS) and deuterated polystyrenes (dPS) were purchased from Pressure Chemical and Polymer Source, respectively, and all used as received (Table 1).

*Corresponding author: Tel 215.898.0593; Fax 215.573.2128; e-mail winey@seas.upenn.edu.

Published on Web 08/18/2009

Table 1. Polymer Characterization of Polystyrene (PS) and Deuterated Polystyrene (dPS) by Size Exclusion Chromatography

name	M_w (kg/mol)	PDI
125k PS	126.4	1.03
480k PS	478.7	1.03
75k dPS	76.9	1.03
140k dPS	137.5	1.03
680k dPS	678.4	1.10

2.2. SWCNT/PS Nanocomposites. SWCNT/PS nanocomposites were prepared by a coagulation method.[23] A SWCNT/*N*, *N*-dimethylformamide (DMF) suspension was bath sonicated for 24 h, mixed with a PS/DMF solution, and sonicated for another 10 s. The SWCNT/PS/DMF suspensions were precipitated in excess water, and the nanocomposites were dried in vacuum (130 °C, 24 h). Our earlier work has used optical microscopy, Raman mapping, and SEM to demonstrate that this fabrication method produces nanocomposites containing uniformly distributed small bundles of SWCNTs.[24,25] Before adding the polymer solution, a SWCNT sample was removed from the SWCNT/DMF suspensions for AFM to find the mean diameter (~9.6 nm) and the mean aspect ratio (~35) of the SWCNT bundles. Coagulation avoids agglomeration of the SWCNT bundles. We report filler concentration in vol % by using the following densities: 1.045 g/cm^3 for PS and 1.3 g/cm^3 for SWCNTs.[26]

The glass transition temperatures (T_g) of 480k PS and all the nanocomposites (ranging from 0.08 to 4 vol % SWCNTs) made with 480k PS were measured using modulated DSC (30−150 °C, 10 °C/min, second run was analyzed). The PS and the nanocomposites exhibit the same T_g, 105 °C. As previously reported, this suggests the absence of strong interaction between the fillers and polymer.[27]

Dynamic frequency sweeps were performed in the linear viscoelastic regime of the composites on a Rheometrics Solid Analyzer (RSAII) using a shear sandwich fixture and a strain of 0.5% at 200 °C in N_2. Studies have previously used rheology to detect a dynamic percolation threshold in SWCNT nanocomposites and suspensions,[17,28,29] because the change from liquidlike to solidlike behavior in the storage modulus indicates the formation of the SWCNT network and percolation. The low-frequency data in Figure 1 for SWCNT/480k PS nanocomposites shows a rheological percolation threshold of 0.24 vol %. These data also show that the polymer relaxation time, which is the inverse of the frequency corresponding to the intersection of the storage modulus and the loss modulus, is constant at ~8 s for 480k PS and the SWCNT/480k PS nanocomposites. Furthermore, the plateau storage moduli at high frequencies are the same for all of the nanocomposites, demonstrating that the entanglement molecular weight (M_e) of the PS in the nanocomposites remains the same with the addition of SWCNTs.[30] The SWCNTs have no substantial influence on the local polymer relaxations in these nanocomposites.

2.3. Preparation of Bilayer Samples. Tracer diffusion experiments used bilayer samples with a PS nanocomposite at the bottom (the matrix) and a thin dPS film on the top (the tracer). The coagulated SWCNT/PS nanocomposites were hot pressed (150 °C) between a silicon wafer and a 4 mm thick glass block to produce smooth films. These thick, nanocomposite films (>40 μm) were annealed for 72 h at 150 °C before assembling the bilayer samples. The dPS top layers were spin-coated on silicon wafers with thicknesses of ~20 nm as characterized by ellipsometry and transferred to the nanocomposite films by standard methods.[15] Bilayer samples were dried (25 °C, 48 h) before isothermally annealing at 150 °C in vacuum to activate the diffusion of dPS into the SWCNT/PS composites. Annealed samples were quenched to room temperature to arrest the polymer diffusion. Given that D was found to be independent of annealing time (as shown below), the annealing time for each bilayer was selected such that the concentration profiles extend 300−500 nm into the matrix and thereby facilitate a rigorous fitting of $\phi(x)$ to determine D.

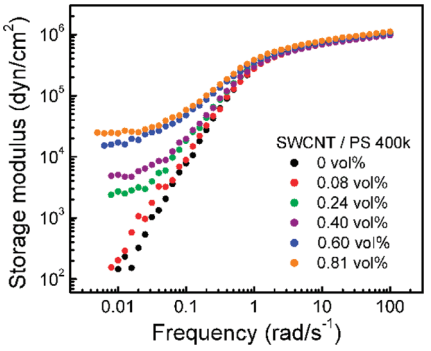

Figure 1. Storage modulus of SWCNT/PS 480k nanocomposites as a function of frequency at various SWCNT concentrations at 200 °C. The relaxation time for local motions remains constant at ~8 s.

2.4. Elastic Recoil Detection (ERD). The concentration profile of dPS in SWCNT/PS nanocomposites was measured by ERD and used to determine the tracer diffusion coefficient.[31] The ERD conditions were He^{2+} (3 MeV) ions, a 15° glancing angle, and a ~5 × 5 mm^2 spot size. ^{1}H and ^{2}D atoms in the sample are scattered in the forward direction and collected by an energy-sensitive detector, such that a count−energy profile is recorded and converted to a dPS volume fraction−depth profile. In these experiments, the ERD sampling depth is ~800 nm and the depth resolution is ~80 nm. The best fits to the ERD data are convolutions of a diffusion equation and a Gaussian function that describes the instrumental resolution.

Numerous researchers have measured polymer tracer diffusion through a matrix of the same polymer and found that when the matrix polymers are highly entangled, the tracer diffusion of entangled chains is found to obey the reptation mechanism.[4] For comparison, Figure 2 shows our experimental tracer diffusion coefficients (D) of dPS in pure PS with data from the literature.[5,14,32] Both our experimental results and selected data from the literature used ERD to determine D and used tracer molecular weights well above the entanglement molecular weight of PS (18 kg/mol).[33] The matrix polymers are well-entangled with molecular weights as follows: 480 kg/mol for this study, 260 and 400 kg/mol for refs 5 and 29, and 2000 kg/mol for ref 14. References 5, 14, and19 reported tracer diffusion coefficients at 174 °C, whereas the experiments in this paper were performed at 150 °C. To facilitate comparison, the $D(T$ = 150 °C) values were shifted to 174 °C using the following equations:

$$\log \frac{D}{T} = A - \frac{B}{T - T_\infty} \tag{1}$$

$$D_2 = D_1 \left(\frac{T_2}{T_1}\right) \exp\left[2.3B\left(\frac{1}{T_1 - T_\infty}\right) - \left(\frac{1}{T_2 - T_\infty}\right)\right] \tag{2}$$

where D_1 and D_2 are the diffusion coefficients at 150 and 174 °C, respectively, T_1 and T_2 are the diffusion temperatures 418 and 447 K, respectively, and the Vogel temperature and constant for polystyrene are T_∞ = 322 K and B = + 983 K.[34] The solid line represents the reptation prediction of $D = D_c/M^2$, where D_c is a constant at fixed T and M is the tracer molecular weight. The D's measured for homopolymers in this study are consistent with literature values.

2.5. Trap Model. As presented below, the minimum in diffusion coefficient as a function of SWCNT concentration could arise due to an anisotropic local diffusion coefficient perpendicular and parallel to the SWCNT. The trap model simulates the changes in the tracer diffusion coefficient by *defining a trap size* and *the extent of slowing perpendicular to the cylindrical trap*. The length of the cylindrical traps is 200 lattice units, and the

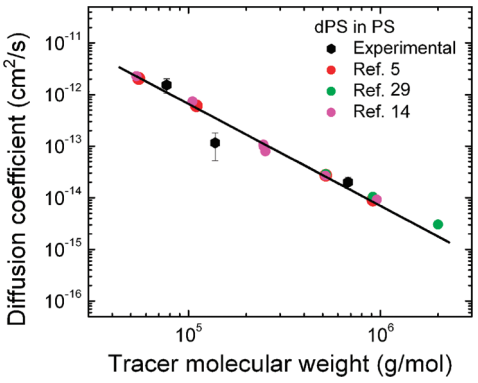

Figure 2. Comparison of our results of dPS diffusion into pure PS with data from literature. The slope of diffusion coefficient versus tracer molecular weight exhibits a −2 slope (solid line), which is consistent with the reptation mechanism.[5,14,32]

radius is either 30 or 40 lattice units. The volume fraction of the cylindrical nanoparticles was calculated using a length and radius of 200 and 3 lattice units, respectively, to be consistent with the mean aspect ratio of the nanotube bundles in the experiments. We randomly place the traps in a 1024^3 lattice cube using periodic boundary conditions and allowing overlap. Note that the simulations were also preformed in a 512^3 lattice cube, and the results are indistinguishable (see Supporting Information). The experimental results suggest that the phenomenon of interest occurs at times and length scales greater than that associated with individual chain motion. Thus, we treat the tracer polymer as a particle and the jump time between lattice sites corresponds to the relaxation time of a chain. The specified jump probabilities (p_0, p_1) dictate the dynamics from one lattice site to another, and the particle motion at steady state determines the global diffusion coefficient. In these initial simulations, the jump probability both outside and inside the trap is $p_0 = 1/6$, while jumps into and out of the traps have a lower probability ($p_1 < p_0$). Each simulation condition was performed five times, and the mean diffusion coefficients are reported. The diffusion coefficient was calculated every 25 000 timesteps for 5000 independent particles, based on the mean-squared number of lattice sites that a particle had diffused from its position at the first time step. The reported diffusion coefficient is the average over 10 such time periods. Simulations were carried out in parallel on an Nvidia Tesla C870 GPU.

3. Results and Discussion

3.1. A Minimum in Polymer Diffusion Coefficient with Increasing SWCNT Concentration. The bilayer films used for ERD have a 20 nm deuterated PS top layer above a thick (>40 μm) SWCNT/PS nanocomposite matrix (Figure 3a, inset). Polymer diffusion occurs upon thermal annealing at 150 °C. After quenching to room temperature, elastic recoil detection was used to determine the dPS concentration profile in the semi-infinite nanocomposite matrix. Figure 3a shows the dPS volume fraction versus depth for 140k dPS diffusing in a 1.6 vol % SWCNT/480k PS matrix. In the as-prepared bilayer, the breadth of the symmetric dPS profile defines the instrumental resolution and determines the total dPS in the bilayer. Upon annealing, the dPS chains penetrate into the matrix and this penetration increases with time. The volume fraction profile for tracer diffusion into a semi-infinite matrix is given by the following solution to Fick's second law[14]

$$\phi(x) = \frac{1}{2}\left[\mathrm{erf}\left(\frac{h-x}{\sqrt{4Dt}}\right) + \mathrm{erf}\left(\frac{h+x}{\sqrt{4Dt}}\right)\right] \qquad (3)$$

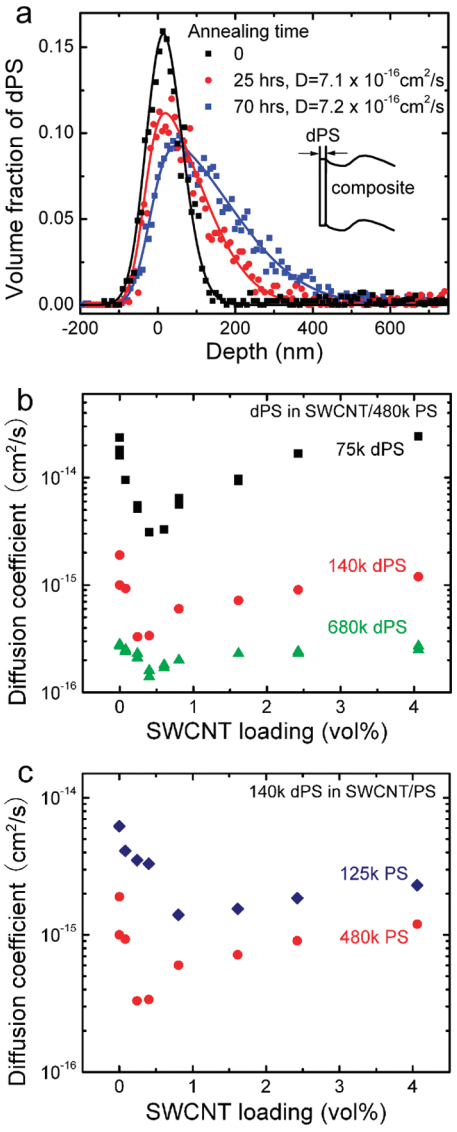

Figure 3. Polymer tracer diffusion in SWCNT/PS nanocomposites measured using ERD. (a) 140k dPS distribution in 1.60 vol % SWCNT/480k PS nanocomposites as prepared and after annealing at 150 °C for different times. The solid lines are fits of the diffusion equation (eq 3) to obtain the diffusion coefficients. Tracer diffusion in these nanocomposites is independent of annealing time. (b) dPS tracer diffusion coefficients in SWCNT/480k PS nanocomposites as a function of SWCNT concentration for three dPS molecular weights. For all dPS, the minimum diffusion coefficient occurs at a SWCNT concentration of 0.4 ± 0.1 vol %. (c) 140k dPS tracer diffusion coefficients at 150 °C as a function of SWCNT concentration in 125k PS and 480k PS nanocomposites. The minimum diffusion coefficient appears at 0.8 vol % SWCNTs in the 125k PS composites.

where $\phi(x)$ is the dPS volume fraction at depth x, h is the thickness of the original dPS layer, t is the diffusion time, D is the tracer diffusion coefficient, and erf denotes the error function. By selecting a D and convoluting $\phi(x)$ with the instrumental resolution, theoretical profiles are fit to the experimental profiles as shown by the solid lines in Figure 3a. The diffusion coefficients of dPS in the SWCNT nanocomposites are the same after 25 h ($D = 7.1 \times 10^{-16}$ cm^2/s) or 70 h ($D = 7.2 \times 10^{-16}$ cm^2/s) of annealing at 150 °C, indicating that the tracer diffusion is independent of annealing time. A constant D also indicates that the SWCNT network in the nanocomposite is constant under these annealing conditions.

The influence of SWCNT concentration on the tracer diffusion coefficient in the SWCNT/480k PS nanocomposites

is shown in Figure 3b. In addition to 140k dPS, D for 75k and 680k dPS as a function of SWCNT volume fraction are given in Figure 3b. At low SWCNT concentrations (ϕ_{SWCNT}), the diffusion coefficient decreases as ϕ_{SWCNT} increases. The diffusion coefficient of the 75k dPS, for example, decreases by almost an order of magnitude, from 1.9×10^{-14} cm^2/s in pure PS to 2.0×10^{-15} cm^2/s in the 0.4 vol % SWCNT composite. In contrast, at higher SWCNT concentrations, D increases as ϕ_{SWCNT} increases. A minimum in the tracer diffusion coefficient (D_{min}) is observed for all the dPS molecular weights investigated. The SWCNT concentration at D_{min} will be called the critical volume fraction (ϕ_{crit}) and is 0.4 ± 0.1 vol % for all three dPS molecular weights in the SWCNT/480k PS nanocomposites. This ϕ_{crit} is in the regime of the observed rheological percolation threshold of these SWCNT/480k PS nanocomposites, 0.24 vol % (Figure 1). At $\phi_{SWCNT} > \phi_{crit}$, D gradually increases from D_{min} toward the tracer diffusion coefficient corresponding to pure PS (D_0). The magnitude of the decrease in D is strongly influenced by the tracer molecular weight, such that a lower dPS molecular weight yields a deeper minimum in D and a smaller D_{min}/D_0.

To explore the importance of matrix molecular weight on tracer diffusion, we performed diffusion studies of the 140k dPS tracer into SWCNT/125k PS nanocomposites. As in the 480k PS nanocomposites, the tracer diffusion of the dPS in 125k PS nanocomposites manifests a rapid decrease followed by a slower increase with the SWCNT loading and exhibits a D_{min} (Figure 3c). As expected, the 140k dPS diffuses faster in 125k PS nanocomposites than in 480k PS nanocomposites.[35] However, the lower molecular weight PS matrix also shifts the critical SWCNT concentration from 0.4 vol % for 480k PS composites to 0.8 vol % for 125k PS composites. Furthermore, the recovery in D at $\phi > \phi_{crit}$ is more gradual for the 125k PS nanocomposites.

In summary, Figure 3 presents dPS tracer diffusion coefficients for four SWCNT/PS nanocomposite systems that show an unprecedented minimum in D as the nanotube loading increases. Across this range of SWCNT concentrations, both the glass transitions temperature from DSC and the relaxation time from linear viscoelastic measurements (Figure 1) are constant. In the reptation model, the diffusion coefficient (D) is given by

$$D = D_0 M^{-2} \tag{4}$$

$$D_0 = \frac{4}{15}\frac{M_0 M_e k_B T}{\xi_0} \tag{5}$$

where M is the tracer molecular weight, M_0 is the monomer molecular weight, M_e is the entanglement molecular weight of the matrix polymer, k_B is the Boltzmann constant, T is temperature, and ξ_0 is the monomeric friction coefficient. In our isothermal diffusion studies where M_0, T, and ξ_0 are expected to remain constant, we can estimate the required change in M_e needed to accomplish the observed D values assuming that the conventional reptation model persists in the presence of nanoparticles. For example, relative to D for 140k dPS in 480k PS, D for 140k dPS in the 0.4 vol % SWCNT/480k PS nanocomposite is smaller by a factor of ~4. This decrease in D corresponds to, on average, a 4-fold decrease in M_e, which further corresponds to a 4-fold increase in the linear viscoelastic plateau modulus, G°_N, according to

$$G^\circ_N = \frac{\rho T N_a k_B}{M_e} \tag{6}$$

where ρ is the polymer density and N_a is Avogadro's number. In contrast, the linear viscoelastic data in Figure 1 for the SWCNT/480k PS nanocomposites show that G°_N is independent of the SWCNT concentration from 0 to 0.8 vol %. Thus, the dependence of the tracer diffusion coefficient on the SWCNT concentration in these nanocomposites is not coupled to changes in the local polymer dynamics of these composites in a manner that is consistent with the simplest reptation model. Moreover, even if M_e of the matrix polymer first decreased and then increased with the addition of SWCNT (as Figure 3b,c would suggest), the reptation model appears inconsistent with tracer molecular dependence of D because the magnitude of the drop in D depends on M. Thus, the observed minimum in the diffusion coefficient with nanoparticle concentration requires us to consider alternative mechanisms.

3.2. Anisotropic Diffusion near SWCNT As Simulated by a Trap Model. Two theories are typically used to describe molecular transport in heterogeneous systems or hybrid materials with impenetrable particles. The Maxwell theory[36] describes how diffusant mobility is impeded by particles acting as obstacles and predicts a monotonic decrease in D, as do extensions of the theory that relax the assumptions of dilute and spherical particles.[37] The free volume theory predicts faster diffusion due to additional free volume associated with the particles and predicts a monotonic increase in D.[38] Neither theory predicts the minimum observed in this study.

We propose that the local diffusion coefficient near the SWCNT is anisotropic such that diffusing perpendicular to the SWCNT is slower than diffusion along the SWCNT (Figure 4a). We will first develop a trap model to simulate the consequences of local anisotropic diffusion on the overall diffusion as a function of filler concentration and then consider our experimental results in light of this model.

We have constructed a phenomenological trap model to simulate the center-of-mass polymer diffusion through a system of cylindrical nanoparticles, wherein the diffusion is anisotropic in the vicinity of nanoparticles. To minimize the number of adjustable parameters, this model defines a trap size and one diffusion asymmetry. The shape of the traps is set by the shape of the nanoparticles (Figure 4a). Figure 4b shows a cylindrical trap (blue) of radius r surrounding a SWCNT (red). Jump probabilities are used to define the center of motion through the three-dimensional lattice. A single jump probability, p_0, is used to described the diffusion both inside and outside the traps; this is consistent with both thermal analysis (T_g) and rheology (relaxation time, plateau modulus) results, indicating that the local dynamics of the matrix polymer are independent of nanoparticle concentration at these loadings. Using a cubic lattice, we set p_0 equal to 1/6. The trap model captures the local anisotropic diffusion by assigning a lower jump probability (p_1) for entering or escaping the trap. This diffusion asymmetry ($p_1 < p_0$) captures the local anisotropic diffusion proposed in Figure 4a by slowing the polymer diffusion only normal to the trap surface.

In contrast to systems with microscale particles, nanoparticle systems possess >10 000 times more specific interfacial area between the particles and the polymer matrix. Furthermore, the volume of the matrix within a radius of gyration of the nanoparticle surface can significantly exceed the volume of the nanoparticles.[39] Similarly, the specific surface area of the traps is large, such that changing the dynamics across the trap boundary alone has a dramatic effect on polymer diffusion. Alternatively, three (matrix, parallel and perpendicular to the filler) or more jump probabilities or even a

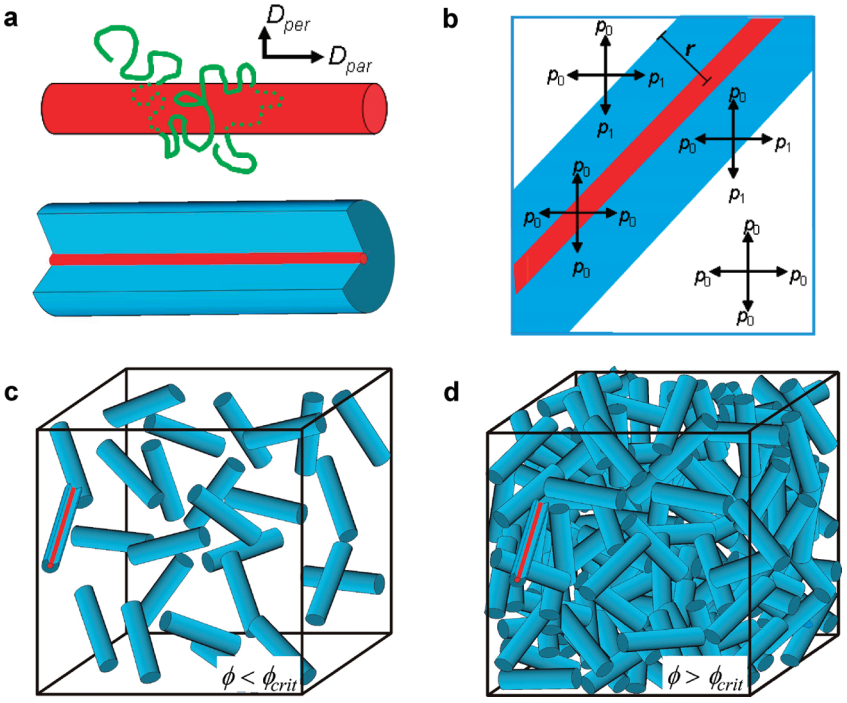

Figure 4. (a) Schematic showing the concept of local anisotropic polymer diffusion of polymers (green) near a nanoparticle (red) whereby the diffusion perpendicular (D_{per}) to the nanoparticle is slower than the diffusion parallel to the nanoparticle (D_{par}). A trap model captures the concept of local anisotropic polymer diffusion by defining a trap (blue) that surrounds the nanoparticle (red). (b) The trap size, as given by the radius of the cylindrical trap, r, determines the spatial extent over which the diffusion is locally anisotropic. The slowing down of the polymer diffusion perpendicular to the trap is represented by assigning a jump probability (p_1) to enter or exit the trap that is smaller than the jump probability inside or outside the trap (p_0), that is, $p_0 > p_1$. (c) At low filler concentrations, $\phi < \phi_{crit}$, the cylindrical traps are below the percolation threshold and diffusion is retarded by the traps. (d) At higher filler concentrations, $\phi > \phi_{crit}$, the cylindrical traps form percolated pathways that allow the diffusion to recover.

gradation in jump probabilities could be used to describe the anisotropic diffusion coefficients near the nanoparticles, but at this stage of the work additional parameters are unwarranted. When the traps are isolated (Figure 4c), polymer movement is slowed (see Figure 5b,d). As the volume fraction of nanoparticles increases, the traps surrounding the particles form a percolating network (Figure 4d). Because (1) polymers move as freely within this network of traps as outside the traps (p_0) and (2) the network spans the entire sample, the influence of the traps on D diminishes above the percolation threshold and D recovers (see Figure 5b,d). By introducing locally anisotropic diffusion coefficients, the simulations using the 3D trap model qualitatively capture the minimum in the tracer diffusion coefficient as a function of nanoparticle concentration, which we also observe experimentally.

3.3. Comparisons of Diffusion Coefficients from Experiments and Trap Model Simulations. Figure 5a replots the experimental diffusion coefficients (Figure 3c) as the normalized diffusion coefficient (D/D_0) for 140k dPS in SWCNT/125k PS and SWCNT/480k PS nanocomposites. A sharper minimum is observed with the larger matrix molecular weight. While D_{min}/D_0 is ~0.20 in both cases, the higher matrix molecular weight exhibits a smaller critical concentration (0.4 vol % rather than 0.8 vol %) and a faster recovery of D/D_0 at $\phi > \phi_{crit}$. Similarly, a sharper minimum is observed when increasing the trap size in the simulations. Figure 5b shows how the simulated D/D_0 values vary with nanoparticle concentration for $p_1 = 0.0001$ and two trap radii, r. As the trap radius increases from 30 to 40 lattice units, the critical volume fraction (ϕ_{crit}) at D_{min}/D_0 decreases from 0.78 to 0.45 vol %. For a fixed nanoparticle size this decrease in ϕ_{crit} with increasing r is expected because increasing r increases the trap volume, such that percolation occurs at a lower ϕ. In these simulations the length of the cylindrical traps is fixed and equal to the nanoparticle length, so increasing the trap radius from 30 to 40 corresponds to increasing the trap volume by 78% at fixed nanoparticle concentration and percolation occurs at a smaller ϕ. Furthermore, the recovery of D/D_0 above ϕ_{crit} is faster for the larger traps. Specifically, although D_{min}/D_0 is comparable for both systems, D/D_0 approaches 1 at ~4 and ~2 vol % for trap radii of 30 and 40, respectively. Overall, the shift to lower ϕ_{crit} and the faster rate recovery for traps with $r = 40$ produces a sharper minimum in D/D_0 relative to the smaller traps. By comparing parts a and b of Figure 5, a strong correlation is revealed between the trap radii and the matrix molecular weight. In SWNCT/PS nanocomposites, we conclude that polymer diffusion is dominated not by the size of the nanoparticles, but rather by the size of the region adjacent to the nanoparticle wherein the local diffusion coefficients are anisotropic. In these SWCNT/PS nanocomposites, the spatial extent of the proposed anisotropic local diffusion is dictated by the matrix molecular weight.

Figure 5c shows the experimental values for D/D_0 as a function of SWCNT concentration where D_{min}/D_0 decreases from 0.55 to 0.18 as the dPS tracer molecular weight decreases from 680k to 75k. Furthermore, the rates of D/D_0 recovery are comparable with D/D_0 approaching 1 at ~4 vol %. Unlike D_{min}/D_0, the critical nanoparticle concentration (ϕ_{crit}) appears to be independent of the tracer molecular weight in the experiments. The trap model simulations produced similar results by changing the probability that a tracer molecule can move in and out of the trap, namely p_1. Figure 5d shows the simulation results, D/D_0, as a function of nanoparticle concentration with $r = 40$. As p_1 decreases from 0.01 to 0.0001, D_{min}/D_0 decreases significantly. Smaller p_1 values indicate greater anisotropy in the local diffusion

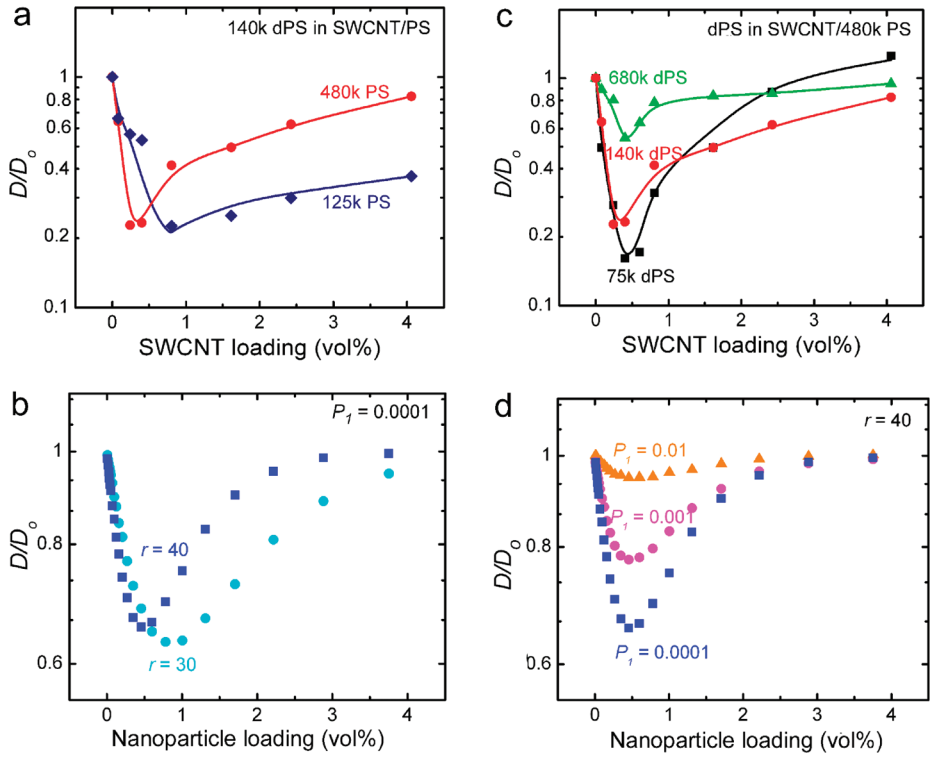

Figure 5. Normalized diffusion coefficients as a function of nanoparticle loading from tracer diffusion experiments and simulations of the trap model. (a) Experimental D/D_0 of 140k dPS diffusing into SWCNT/PS nanocomposites with PS matrix molecular weights of 125k and 480k. (b) Simulated D/D_0 from the trap model with $p_1 = 0.0001$ and two trap sizes of $r = 30$ or $r = 40$ lattice units. (c) Experimental D/D_0 of dPS in SWCNT/480k PS nanocomposites for three tracer molecular weights. (d) Simulated D/D_0 from the trap model having $r = 40$ lattice unit and various jump probabilities, p_1. In all simulations, $p_0 = 0.167$ and the trap length is 200 lattice units. The nanoparticle loading is calculated using a filler radius of 3 lattice units.

coefficients, making is more difficult to enter or escape from the trap relative to diffusing within the trap or in the matrix (p_0). By comparing the experimental and simulations results, we found that in these SWCNT/PS nanocomposites the small tracer molecules correlated with greater diffusional anisotropy.

3.5. Discussion. We report a minimum in the tracer diffusion coefficient as the nanoparticle concentration increases in polymer composites with cylindrical (1D) nanoparticles, namely SWCNTs. This previously unreported phenomenon results, at least in part, from the new size regime that is now available by the synthesis of particles that are smaller than the polymers. Nanoparticles give rise to polymer nanocomposites with much larger specific interfacial areas, such that even a modest perturbation in the vicinity of the nanoparticles can have significant ramifications on the observed polymer properties. Furthermore, this phenomenon might have relevance beyond polymer nanocomposites, in that living organisms require macromolecule diffusion in the vicinity of natural nanoparticles including globular proteins and actin filaments.

The minimum in the diffusion coefficient is inconsistent with a simple reptation model; for example, the significant changes in D are not coupled with changes in M_e. However, we were able to capture the tracer diffusion results by imposing an anisotropic diffusion coefficient in the vicinity of the nanoparticles, as simulated by the trap model. The physical origin of this locally anisotropic diffusion requires additional theoretical, computational, and experimental work in a variety of nanoparticle/polymer systems. A possible physical interpretation of the anisotropic diffusion could involve a disruption of polymer reptation near nanoparticles. Reptation describes the motion of a polymer chain along a confining tube that is defined by constraints or entanglements within a high molecular weight polymer melt. With sufficient thermal energy and time the entanglements that define the confining tube relax because these entangled polymers have diffused out of their own tubes. Perhaps, in the vicinity of nanoparticles, the confining tube for polymer reptation is perturbed such that diffusion becomes locally anisotropic. Certainly, in these SWCNT/PS nanocomposites the SWCNT bundles are non-Brownian at 150 °C, such that any perturbation involving a SWCNT bundle will be long-lived compared to confining tubes defined solely by the polymer matrix. We have several studies underway that are designed to determine the range of materials showing a minimum in the diffusion coefficient with nanoparticle concentration and to ascertain the underlying polymer physics.

4. Conclusion

Polymer diffusion in polymer nanocomposites containing SWCNT consistently shows an initial decrease in the tracer diffusion coefficient, D, followed by a recovery of D upon increasing nanotube concentration. We have proposed that this minimum in D arises from anisotropic diffusion coefficients near the nanoparticles and simulated the influence of this anisotropy using a 3D trap model. Strong correlations were found between the SWCNT/PS nanocomposites and simulations of the trap model showing that (i) as the matrix molecular weight increases the anisotropic diffusion persists at greater distances from the filler and (ii) as the tracer molecular weight decreases the difference in diffusion perpendicular and parallel to the filler becomes greater. The discovery of a minimum in diffusion coefficient with nanoparticle concentration is unexpected and is important for the fabrication, processing, and application of polymer nanocomposites and the extension of reptation models.

Acknowledgment. This research was funded by the National Science Foundation MRSEC-DMR05-20020 (K.I.W., R.J.C.) and Polymer Programs DMR05-49307(RJC). N.C. gratefully acknowledges the award of an Overseas Travel Grant, EP/E050794/1, from the EPSRC. The authors gratefully acknowledge the use of the size exclusion chromatograph in Prof. Shu Yang's laboratory at the University of Pennsylvania. The authors thank Sadie White for valuable discussions and Dr. Chen Xu and Dr. Doug Yates for assistance with the experiments.

Supporting Information Available: Comparison of the trap model simulation results for 512^3 and 1024^3 simulation volumes, wherein the normalized diffusion coefficient is unchanged. This material is available free of charge via the Internet at http://pubs.acs.org

References and Notes

(1) Fick, A. *Philos. Mag.* **1855**, *10*, 30–39.
(2) Fick, A. *Poggendorff's Ann. Phys.* **1855**, *94*, 59–86.
(3) Einstein, A. *Ann. Phys.* (*Leipzig*) **1906**, *19*, 371–381.
(4) de Gennes, P. G. *J. Chem. Phys.* **1971**, *55* (2), 572–579.
(5) Green, P. F.; Mills, P. J.; Palmstrom, C. J.; Mayer, J. W.; Kramer, E. J. *Phys. Rev. Lett.* **1984**, *53* (22), 2145–2148.
(6) Lodge, T. P. *Phys. Rev. Lett.* **1999**, *83* (16), 3218–3221.
(7) McLeish, T. *Phys. Today* **2008**, *61* (8), 40–45.
(8) Kapnistos, M.; Lang, M.; Vlassopoulos, D.; Pyckhout-Hintzen, W.; Richter, D.; Cho, D.; Chang, T.; Rubinstein, M. *Nat. Mater.* **2008**, *7* (12), 997–1002.
(9) Clarke, N.; Colley, F. R.; Collins, S. A.; Hutchings, L. R.; Thompson, R. L. *Macromolecules* **2006**, *39* (3), 1290–1296.
(10) Lodge, T. P.; Dalvi, M. C. *Phys. Rev. Lett.* **1995**, *75* (4), 657–660.
(11) Vaia, R. A.; Ishii, H.; Giannelis, E. P. *Chem. Mater.* **1993**, *5* (12), 1694–1696.
(12) McWilliams, A. NANO21C, BCC Research, Norwalk, **2006**.
(13) Ajayan, P. M.; Schadler, L. S.; Braun, P. V. *Nanocomposite Science and Technology*; Wiley-VCH: Weinheim, 2003.
(14) Mills, P. J.; Green, P. F.; Palmstrom, C. J.; Mayer, J. W.; Kramer, E. J. *J. Polym. Sci., Part B: Polym. Phys.* **1986**, *24* (1), 1–9.
(15) Composto, R. J.; Kramer, E. J.; White, D. M. *Nature* **1987**, *328* (6127), 234–236.
(16) Vonseggern, J.; Klotz, S.; Cantow, H. J. *Macromolecules* **1991**, *24* (11), 3300–3303.
(17) Du, F. M.; Scogna, R. C.; Zhou, W.; Brand, S.; Fischer, J. E.; Winey, K. I. *Macromolecules* **2004**, *37* (24), 9048–9055.
(18) Hinds, B. J.; Chopra, N.; Rantell, T.; Andrews, R.; Gavalas, V.; Bachas, L. G. *Science* **2004**, *303* (5654), 62–65.
(19) Holt, J. K.; Park, H. G.; Wang, Y. M.; Stadermann, M.; Artyukhin, A. B.; Grigoropoulos, C. P.; Noy, A.; Bakajin, O. *Science* **2006**, *312* (5776), 1034–1037.
(20) Elf, J.; Li, G. W.; Xie, X. S. *Science* **2007**, *316* (5828), 1191–1194.
(21) Konopka, M. C.; Sochacki, K. A.; Bratton, B. P.; Shkel, I. A.; Record, M. T.; Weisshaar, J. C. *J. Bacteriol.* **2009**, *191* (1), 231–237.
(22) Zhou, W.; Ooi, Y. H.; Russo, R.; Papanek, P.; Luzzi, D. E.; Fischer, J. E.; Bronikowski, M. J.; Willis, P. A.; Smalley, R. E. *Chem. Phys. Lett.* **2001**, *350* (1−2), 6–14.
(23) Du, F. M.; Fischer, J. E.; Winey, K. I. *J. Polym. Sci., Part B: Polym. Phys.* **2003**, *41* (24), 3333–3338.
(24) Du, F.; Scogna, R. C.; Zhou, W.; Brand, S.; Fischer, J. E.; Winey, K. I. *Macromolecules* **2004**, *37* (24), 9048–9055.
(25) Mu, M.; Winey, K. I. *J. Phys. Chem. C* **2007**, *111* (48), 17923–17927.
(26) Thess, A.; Lee, R.; Nikolaev, P.; Dai, H.; Petit, P.; Robert, J.; Xu, C.; Lee, Y. H.; Kim, S. G.; Rinzler, A. G.; Colbert, D. T.; Scuseria, G. E.; Tománek, D.; Fischer, J. E.; Smalley, R. E. *Science* **1996**, *273* (5274), 483–487.
(27) Rittigstein, P.; Torkelson, J. M. *J. Polym. Sci., Part B* **2006**, *44* (20), 2935–2943.
(28) Kashiwagi, T.; Du, F. M.; Douglas, J. F.; Winey, K. I.; Harris, R. H.; Shields, J. R. *Nat. Mater.* **2005**, *4* (12), 928–933.
(29) Hough, L. A.; Islam, M. F.; Janmey, P. A.; Yodh, A. G. *Phys. Rev. Lett.* **2004**, *93* (16), 168102.
(30) Composto, R. J.; Kramer, E. J.; White, D. M. *Macromolecules* **1992**, *25* (16), 4167–4174.
(31) Composto, R. J.; Walters, R. M.; Genzer, J. *Mater. Sci. Eng. R* **2002**, *38* (3−4), 107–180.
(32) Green, P. F.; Kramer, E. J. *Macromolecules* **1986**, *19* (4), 1108–1114.
(33) Ferry, J. *Viscoelastic Properties of Polymers*; Academic Press: New York, 1980.
(34) Green, P. F.; Kramer, E. J. *J. Mater. Res.* **1986**, *1* (1), 202.
(35) Wang, S. Q. *J. Polym. Sci., Part B: Polym. Phys.* **2003**, *41* (14), 1589–1604.
(36) Maxwell, C. *Treatise on Electricity and Magnetism*; Oxford University Press: London, 1983; Vol. *1*.
(37) Crank, J. *The Mathematics of Diffusion*, 2nd ed.; Oxford University Press: London, 1975.
(38) Hill, R. J. *Phys. Rev. Lett.* **2006**, *96* (21), 216001.
(39) Winey, K. I.; Vaia, R. A. *MRS Bull.* **2007**, *32* (4), 314–319.